

Direct Detection Antenna-Coupled mmW Sensors for the Detection of Explosive Vapors

Michael Gritz^a, Rafael Hernandez^b, Eli Gordon^a, Amedeo Larussi^b, Guy Zummo^c, Glenn Boreman^c, and Leonard Chen^a

^aRaytheon, Network Centric Systems, Raytheon Vision Systems, 75 Coromar Dr., Goleta, CA USA 93117 (michael_a_gritz@raytheon.com)

^bRaytheon, Space and Airborne Systems, Electronic Warfare Systems, 6380 Hollister Ave, Goleta, CA 93117

^cCREOL/School of Optics, University of Central Florida, Orlando FL 32816 (email: boreman@creol.ucf.edu)

ABSTRACT

The low vapor pressure and concentration of explosive such as TNT and RDX pose significant problems for the detection of explosive vapors in the mmW bands. For the positive identification of explosive vapors using an uncooled passive mmW imaging spectrometer with a low false alarm rate (FAR) requires an unprecedented sensitivity of <150 fW. We report on the recent development of a novel uncooled mmW antenna-coupled direct detector, which shows promise of meeting this requirement.

Keywords: antenna-coupled detectors, wavelength tunable detectors, passive mmW imaging

1. INTRODUCTION

Our antenna-coupled direct detector works by collecting the incident electro-magnetic radiation with a scalable, planar lithographic antenna element. The collected radiation is directly injected into the sensor electronics, which rectify the signal. The rectification of the radiation is achieved by using a GaAs Schottky diode to convert the high frequency input signal to DC power. Using advanced semiconductor processing, Raytheon fabricated GaAs Schottky diodes integrated with a half-wave dipole antennas with a measured noise-equivalent-temperature difference (NETD) of 20K at room temperature. Additional improvements on the antenna design indicate that the direct combination of an optimum antenna design with our Schottky diode enables unprecedented sensitivities in the <150 fW range (<1K NETD).

Furthermore our technology is capable of being implemented as a "spectrometer on a chip" by using existing frequency agile technology previously demonstrated at the University of Central Florida/CREOL in the long wave infrared (LWIR) by the author¹.

In this work, we present the measured spectral response from 75 to 140 GHz on a passive mmW antenna-coupled direct detector. The measured NETD and the noise-equivalent-power (NEP) using two different testing methodologies will also be presented. The detector measurements presented here serve mainly to place bounds on necessary detector requirements for the detection of explosive vapor.

2. EXPERIMENTAL DETAILS

A proof-of-concept (POC) antenna-coupled mmW detector was built by combining an optimum antenna design with a commercially off the shelf (COTS) Schottky diode. A photo of the detector integrated with a set of dipole antenna is shown in Figure 1. The novelty of our device is that it is a spectrally tunable LC resonator circuit with a high Q-factor, which is capable of scaling to higher frequencies by simply changing the size of our antenna element without any loss of sensitivity.

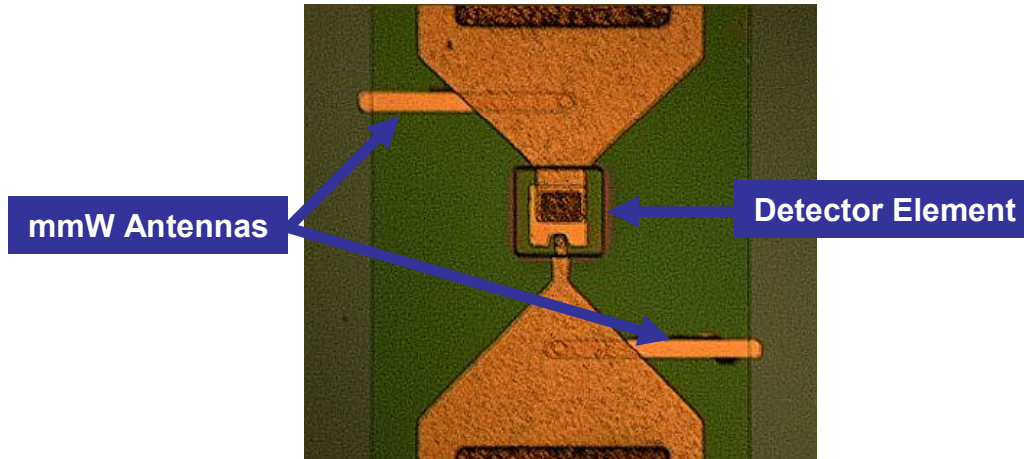


Figure 1. Schematic of the set up used to measure the spectral responsivity and NEP of the antenna-coupled direct detector.

Additional processing steps are required to prepare the substrates to be measured. The processing begins with a quarter of a three-inch GaAs substrate, which is completely patterned with Schottky diodes. The major steps of the process are (1) scribing the substrate into a 1cm x 1cm piece, (2) surface clean-up, (3) epoxy the substrate to a ceramic chip carrier, and (4) aluminum wire-bonding.

Upon completion of the wire-bonding, the detectors were characterized using two independent testing methodologies. For the first test case, a tunable vector network analyzer (VNA) with a NIST calibrated power meter was used to determine the spectral response of the detectors and the NEP (see Figure 2). The second case an extended source infrared (IR) blackbody with a measured emissivity (ϵ) in the mwW was used to determine the NETD of the detector (see Figure 3).

For the first the spectral response of the transmitter must be determined. This is accomplished by measuring the power emitted from the source in Watts from 90 to 140 GHz in 5 GHz steps using a tunable vector network analyzer (VNA) with a NIST calibrated power meter. The power meter is equipped with an equivalent sized horn antenna used in the test setup to measure the detectors. The VNA transmitter was equipped with 16° beam width conical horn antenna. The polarization was horizontal. To change the polarization we changed the orientation of the power meter. The beam was modulated with a chopper at a frequency of 200 Hz. The power meter was placed 3mm away from the chopper in the center of the beam. The measured power (P) was observed to be the same for both polarizations.

To measure the spectral response of the detector, the VNA transmitter was equipped with 16° beam width conical horn antenna. An outline of the test set-up is displayed in Figure 2. The polarization was horizontal. To change the polarization we changed the orientation of the device under test (DUT).

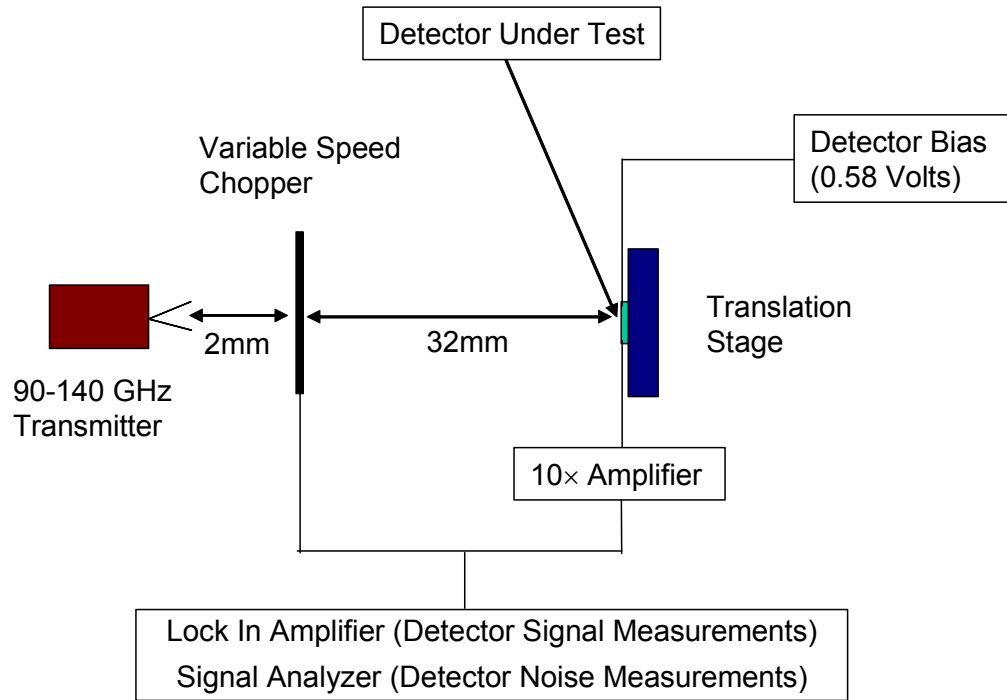


Figure 2. Schematic of the set up used to measure the spectral responsivity and NEP of the antenna-coupled direct detector.

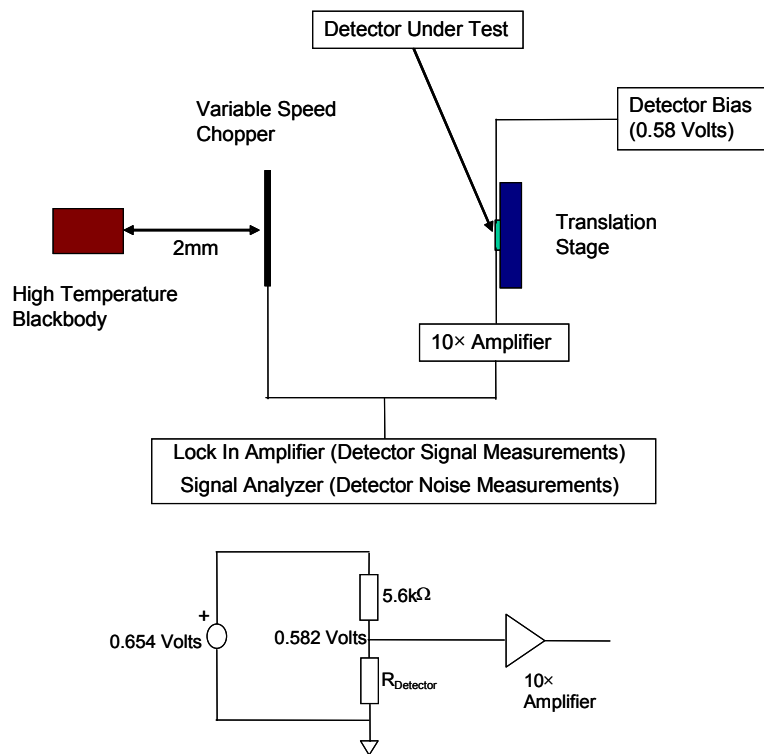


Figure 3. Schematic of the set up used to measure the NETD of the antenna-coupled direct detector.

3. RESULTS

The DUT was placed in the center of the beam. The position of the device was adjusted for the best response by using optical translation stages. The device was measured with a bias of 580 mVolts. The beam was modulated with a chopper at a frequency of 200 Hz. The modulated signal was read with a lock in amplifier after a 10× pre-amplification. For the device under test, the signal $V_{BondPad}$ was obtained for the polarization parallel to the antenna axis and the minimum signal V_{Dipole} for the cross polarization in 5 GHz steps from 90 to 140 GHz.

The NEP in picowatts ($\text{fW}/\text{Hz}^{1/2}$) is determined as follows:

$$NEP = \frac{V_N}{\mathfrak{R}} 1 \times 10^{12} \quad (1)$$

where:

P_D is the power density on the detector (Watts/cm^2)

A_D is the effective area of the detector (cm^2)

V_S is the output voltage signal (Volts)

V_N is the noise floor voltage signal (Volts)

\mathfrak{R} is the responsivity of the detector (Volts/Watt)

In order to determine the NEP of our detector, we measured the noise level of our device using a signal analyzer with a 5kHz bandwidth. The measurements were taken while the device was biased with no power being emitted from the VNA transmitter. The measured noise floor was $90 \text{ nV}/\text{Hz}^{1/2}$. In an antenna-coupled direct detector, the effective area is determined by measuring the antenna directivity of the DUT^{2,3}. Since the test equipment used cannot measure the directivity of the antenna, the effective area was calculated assuming an ideal dipole antenna using:

$$A_D = \frac{0.26\lambda^2}{2} \quad (2)$$

where:

λ is the free space wavelength

The results of the measurement in both polarizations are displayed in Table 1. . Using the results presented in Table 1 the median NEP is $61.6 \text{ pW}/\text{Hz}^{1/2}$. Using the set-up displayed in Figure 3, the NETD of the antenna-coupled direct detectors is 20K

Table 1. Spectral response of the detector.

Freq (GHz)	Measured Signal Vertical Polarization (Volts - rms)	Measured Signal Horizontal Polarization (Volts - rms)	Measured Power Density (Watts per cm^2)	NEP - Vertical Polarization ($\text{pW}/\text{Hz}^{1/2}$)	NEP - Horizontal Polarization ($\text{pW}/\text{Hz}^{1/2}$)
90	1.43E-03	1.32E-03	5.97E-06	3.45E-11	3.75E-11
95	1.35E-03	7.00E-04	1.13E-05	6.91E-11	1.34E-10
100	1.26E-03	6.59E-04	8.92E-06	5.85E-11	1.12E-10
105	2.72E-03	1.33E-03	1.27E-05	3.87E-11	7.90E-11
110	1.29E-03	2.42E-04	9.63E-06	6.16E-11	3.29E-10
115	7.30E-04	2.03E-04	9.00E-06	1.02E-10	3.67E-10
120	2.23E-04	1.28E-04	6.05E-06	2.24E-10	3.91E-10
125	3.45E-04	1.70E-04	7.16E-06	1.72E-10	3.49E-10
130	2.40E-04	8.86E-05	1.83E-06	6.31E-11	1.71E-10
135	4.44E-04	2.66E-04	3.03E-06	5.64E-11	9.42E-11
140	1.17E-04	6.41E-05	7.16E-07	5.06E-11	9.25E-11

3.1 Spectral Measurements of Solid TNT

Fig. 4 presents the spectrum of solid TNT in the range 30-660 cm^{-1} at resolution 1 cm^{-1} . We find in Fig. 4 all previously reported lines, namely those at 123, 157, 186, 272, 305, 325, 355, 453, 603, and 639 cm^{-1} . However, we are able to resolve more structure in our spectrum. For example, the strong 350 cm^{-1} line is here revealed to be a doublet. We find a previously unreported line at 525 cm^{-1} , and the lines revealed below 100 cm^{-1} in Fig. 4 (right) are apparently new.

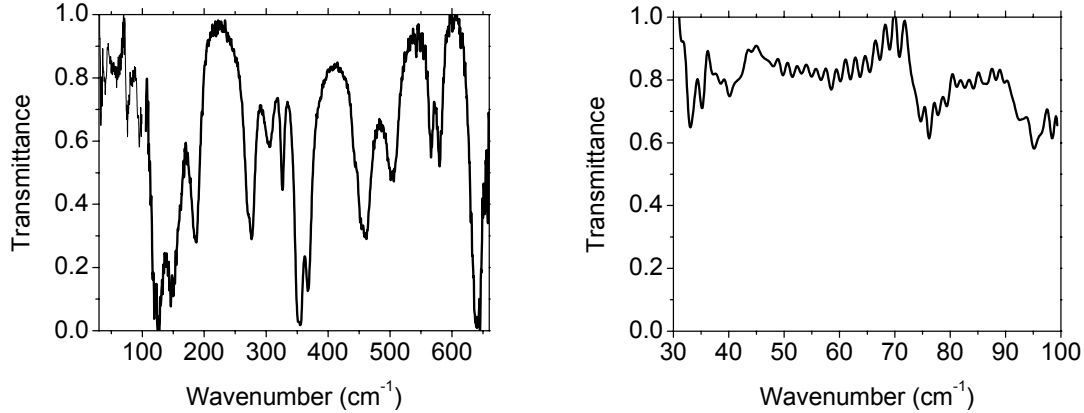


Figure 4. (left) Far-IR spectrum of ~ 0.1 mm thick sample of solid TNT. (right) Detail of long wave portion showing weak absorption features. The fast oscillations are Fabry-Perot resonances in the polyethylene substrate, and the broad derivative-like structure near 70 cm^{-1} is likewise an artifact due to a polyethylene absorption band.

As an example calculation of the absorption cross section, we consider the line in Fig. 4 at ~ 275 cm^{-1} . The minimum transmittance is 0.3, giving an absorbance value of 1.2, and with a 0.1 mm sample thickness, the absorption coefficient is found to be 120 cm^{-1} . Using the concentration of molecules in the solid gives an absorption cross section of about 2.7×10^{-20} cm^2 .

4. SUMMARY

The measured spectral response from 75 to 140 GHz on a passive mmW antenna-coupled direct detector has been measured. The NETD and the noise-equivalent-power (NEP) using two different testing methodologies were found to be 20K and in the pW range. The measured transmittance spectra of TNT solid in the range 30-660 cm^{-1} enables the absorption cross-section to be determined.

REFERENCES

1. M. Gritz, M. Metzler, M. Abdel-Rahman, B. Monacelli, G. Zummo, D. Malocha, and G. Boreman, "Characterization of a wavelength-tunable antenna-coupled infrared microbolometer" *Optical Engineering*, 44, (2005).
2. J. Alda, C. Fumeaux, I. Codreanu, J. Schaefer, and G. Boreman, "A deconvolution method for two-dimensional spatial response mapping of lithographic infrared antennas", *Applied Optics*, 38, 3993-4000 (1999).
3. C. Fumeaux, M. Gritz, I. Codreanu, W. Schaich, F.J. Gonzalez, and G. Boreman, "Measurements of the resonant lengths of infrared dipole antennas," *Infrared Physics and Technology*, 41, 271-281 (2000).